p21 Downregulation is an important component of PAX3/FKHR oncogenicity and its reactivation by HDAC inhibitors enhances combination treatment

Hecker, R M ; Amstutz, R A ; Wachtel, M ; Walter, D ; Niggli, F K ; Schäfer, B W

Abstract: A number of drugs developed against cancer-specific molecular targets have been shown to offer survival benefits alone or in combination with standard treatments, especially for those cases in which tumor pathogenesis is dominated by a single molecular abnormality. One example for such a tumor type is alveolar rhabdomyosarcoma (aRMS), which is characterized by a specific translocation creating the oncogenic PAX3/FKHR transcription factor, believed to be the molecular basis of the disease. Recently, we were able to show that the small molecule inhibitor PKC412 (midostaurin) shows strong antitumor activity against aRMS by reducing the transcriptional activity of PAX3/FKHR. In this study, we screened for combination strategies that are superior to PKC412-only treatment and found that the combination of PKC412 with histone deacetylase inhibitors like valproic acid (VPA) synergistically induced apoptosis resulting in suppressed aRMS tumor growth in vivo. We provide evidence that the antitumor effect on combination treatment is achieved by VPA-induced reactivation of p21, which is downregulated in aRMS cells by destabilization of the transcriptional regulator EGR1 by PAX3/FKHR. Our study highlights a possible mechanism behind the increased efficacy and indicates that different arms of PAX3/FKHR oncogenicity can be exploited therapeutically by the specific combination of drugs to increase their therapeutic potential.

DOI: https://doi.org/10.1038/onc.2010.145

p21 Downregulation is an Important Component of PAX3/FKHR Oncogenicity and its Reactivation by HDAC Inhibitors Enhances Combination Treatment

Regina M. Hecker[1], Ralf A. Amstutz[1], Marco Wachtel[1], Dagmar Walter[1], Felix K. Niggli[1] and Beat W. Schäfer[1,2]

[1]Department of Oncology, University Children's Hospital Zurich, Steinwiesstrasse 75, CH-8032 Zurich Switzerland

[2]To whom requests for reprints should be addressed, at Department of Oncology, University Children's Hospital, Steinwiesstrasse 75, CH-8032 Zurich, Switzerland. Phone: 0041 44 266 75 53, Fax: 0041 44 266 71 71, E-mail: beat.schaefer@kispi.uzh.ch

Running title: Downregulation of p21 by PAX3/FKHR

This study was supported by grants (3100-109837 and 3100-122562) from the Swiss National Science Foundation (SNF).

Abstract

A number of drugs developed against cancer-specific molecular targets have been shown to offer survival benefits alone or in combination with standard treatments, especially for those cases where tumor pathogenesis is dominated by a single molecular abnormality. One example for such a tumor type is alveolar rhabdomyosarcoma (aRMS) which is characterized by a specific translocation creating the oncogenic PAX3/FKHR transcription factor, believed to be the molecular basis of the disease. Recently, we were able to demonstrate that the small molecule inhibitor PKC412 (midostaurin) exhibits strong antitumor activity against aRMS by reducing the transcriptional activity of PAX3/FKHR.

Here, we screened for combination strategies that are superior to PKC412-only treatment and found that the combination of PKC412 with histone deacetylase (HDAC) inhibitors like valproic acid (VPA) synergistically induced apoptosis resulting in suppressed aRMS tumor growth *in vivo*.

We provide evidence that the antitumor effect upon combination treatment is achieved by VPA-induced reactivation of p21 which is downregulated in aRMS cells via destabilization of the transcriptional regulator EGR1 by PAX3/FKHR. Our study highlights a possible mechanism behind the increased efficacy and indicates that different arms of PAX3/FKHR oncogenicity can be exploited therapeutically by the specific combination of drugs to increase their therapeutic potential.

Key words: Rhabdomyosarcoma, PAX3/FKHR, p21, combination treatment

Introduction

The phenomenon of oncogene addiction allows the development of targeted therapies for poor-outcome malignancies whereby the clinical success of kinase inhibitors such as imatinib demonstrate the feasibility of such an approach. However, clinical experience also indicates that the risk of outgrowth of therapy-resistant subclones with single agent treatments is rather high and their efficacy can be very limited. Hence, and given the vast number of agents in pre-clinical development, one of the big challenges ahead will be to define rational combination treatments that show the most promising clinical benefit. Such combinations might be directed against one signalling pathway at different molecular levels or target complementary pathways to achieve maximal efficacy.

As a model to explore such possibilities we use the pediatric sarcoma rhabdomyosarcoma (RMS). RMS is the most common pediatric soft tissue cancer and accounts for about 5-8% of all malignancies in children (Merlino and Helman, 1999). Histopathologically, two main subtypes of RMS, embryonal RMS (eRMS) and alveolar RMS (aRMS) can be distinguished. While eRMS has a favourable prognosis with survival rates of up to 94 % for the most favourable subgroups, the aRMS histotype is associated with poor survival rates of 30 % only as aRMS occurs at unfavourable sites and demonstrates a highly malignant phenotype (Meyer and Spunt, 2004). Also within the stratified patient cohort of metastatic RMS with two or fewer metastatic sites, non-embryonal histology is associated with an unfavourable prognosis while embryonal histology contributes significantly to better prognosis, with 21% and 40% of failure-free survival, respectively (Breneman *et al.*, 2003). Dose intensification and the use of multiagent chemotherapy offer only very modest survival benefits for children with disseminated or recurrent disease and unfavourable RMS histology (Pappo *et al.*, 1999; Smith *et al.*, 2001). Therefore, new therapeutic strategies are urgently needed for such high-risk patients.

The majority of aRMS cases is associated with the chromosomal translocation t(2;13) generating the PAX3/FKHR fusion protein. This chimeric transcription factor contains the two DNA binding domains of PAX3 and the transactivation domain derived from FKHR, also known as FOXO1A. As PAX3/FKHR is a stronger transactivator than its wild-type counterpart, it has been suggested that the oncogenic potential of the fusion results from dysregulation of PAX3 target genes. Established aRMS tumors are dependent on continuous expression of PAX3/FKHR similar to multiple examples of cancers that show to be addicted to certain activated oncogenes. Hence, these tumor-specific oncogenic transcription factors represent an ideal therapeutic target for the development of novel therapeutic strategies.

Along these lines, we recently reported that the kinase inhibitor PKC412 (midostaurin) can influence the oncogenic activity of PAX3/FKHR through modulation of specific phosphorylation sites within the PAX3 domain (Amstutz *et al.*, 2008). Phosphorylation at these sites was shown to perturb efficient DNA-binding. Consequently, treatment of aRMS with PKC412 resulted in potent antitumoral effects both *in vitro* as well as *in vivo*.

Apart from this well-investigated oncogenic activity at the level of direct target gene activation, PAX3/FKHR also exerts a repressive effect that has been less well characterized. Recently, it has been reported that PAX3/FKHR has a protein-destabilization effect (Roeb *et al.*, 2007), as PAX3/FKHR was shown to directly interact with the early growth responsive transcription factor EGR1 thereby targeting EGR1for proteasomal degradation. EGR1 plays important roles in regulating cell growth, differentiation and development (Liu *et al.*, 1996) and has been shown to mediate expression of p57Kip2 as one of its target genes.

Here we demonstrate that degradation of EGR1 by PAX3/FKHR leads to the repression of the tumor suppressor and cell cycle regulator p21 and thereby identify *p21* as a novel gene that is repressed by PAX3/FKHR.

In an attempt to find substances synergistic with PKC412 in their ability to inhibit aRMS cell proliferation, we found that reactivation of p21 expression by HDAC inhibitors strongly augments PKC412-mediated apoptosis in aRMS cells, *in vitro* and *in vivo*. These findings highlight the complexity of aRMS tumor pathogenesis created by the translocation positive genotype and provide the basis for a evidence-based combination treatment of aRMS with PKC412 and HDAC inhibitors to exert a therapeutic benefit by targeting different arms of PAX3/FKHR oncogenicity.

RESULTS

Combination of PKC412 with VPA leads to synergistic antitumor activity on aRMS cells *in vitro* through reactivation of p21 expression levels.

We recently identified PKC412 as a potent antitumorigenic agent for aRMS treatment *in vitro* and *in vivo (Amstutz et al., 2008)*. To further increase treatment efficacy, we performed *in vitro* combination studies with chemotherapeutic agents used in RMS therapy or HDAC inhibitors which have been shown to act synergistically with PKC412 against acute myelogenous leukaemia (AML) (Bali *et al.*, 2004). IC_{50} values of these agents were determined in aRMS cell lines RH4 and RH30 either as single agents or in combination with 50nM PKC412, a concentration which is about 10 times below its IC_{50} and thus only has a marginal influence on cell viability by itself. To evaluate synergistic effects, a combination index (CI) was calculated which is the IC_{50} ratio between combined and single treatments and which indicates synergism at a value <1. Strong synergistic effects with CI values of 0.48 and 0.61 were observed in RH4 cells for both HDAC inhibitors, VPA and SAHA, whereas from the chemotherapeutic compounds only vincistrine showed weak synergism in combination with PKC412. In RH30 cells, all compounds tested showed some synergistic effects with PKC412. Similar to RH4 cells, the lowest CI value could be detected upon cotreatment with VPA (Figure 1a). These results suggest a rationale for combining PKC412 and HDAC inhibitors, especially VPA, and prompted us to further investigate this combination for treatment of aRMS.

To confirm VPA as a combination partner for PKC412, we next determined whether cotreatment with clinical applicable concentrations of VPA would sensitize aRMS cells to cell death induced with IC_{50} concentrations of PKC412. As expected, single treatment with 0.5µM PKC412 resulted in a strong induction of cell death for both aRMS cell lines. By itself, VPA exerted no cytotoxicity following 72h of continuous exposure to 1mM. However, cotreatment with 1mM VPA dramatically enhanced PKC412-induced cell death, indicating synergistic antitumoral activity on aRMS cells (Figure 1b).

As PKC412 induced cell death is due to caspase-3-dependent apoptosis (Amstutz *et al.*, 2008), we tested whether VPA might further enhance apoptosis by an activated caspase-3 assay. This revealed an at least 2-fold increase in the number of apoptotic cells in combined treatment compared to PKC412 single treatment (Figures 2a and b). RH4 cells showed an increased apoptotic response compared to RH30 cells, with values of 50.8% and 42.5% respectively, consistent with the observed stronger induction of cell death for these cells.

To further confirm these findings we monitored PARP cleavage in cells treated with drugs from 2 to 16h by Western blot analysis. In both aRMS cell lines time-dependent increase in PARP cleavage was more pronounced after combination treatment compared to either single treatment alone (Figure 2c). In addition to VPA we observed that also other HDAC inhibitors like sodium butyrate or SAHA (Figures 1a, b and data not shown) can act in combination with PKC412 to mediate an enhanced reduction of aRMS cell viability. Taken together, these results clearly show that HDAC inhibitors synergize with PKC412 to enhance apoptosis in aRMS cells. Since different HDAC inhibitors have a similar synergistic effect, their mode of action is likely to rely on a class-specific mechanism.

One very prominent effect observed for a large panel of HDAC inhibitors is induction of p21 (Archer *et al.*, 1998; Kim *et al.*, 2001; Sowa *et al.*, 1997; Wilson *et al.*, 2006). Hence, we determined p21 expression levels upon HDAC inhibitor treatment alone and in combination with PKC412. p21 protein levels were significantly upregulated upon HDAC inhibitor treatment irrespective of additional treatment with PKC412 (Figure 2d and Supplementary Figure S1a). This is true for both aRMS cell lines RH4 and RH30, which demonstrate similar levels of PAX3/FKHR expression (Supplementary Figure S1b) and are either deleted in *p53* or carry *p53* mutations (Barlow *et al.*, 2006), thereby excluding a role of p53 in p21 promoter activation.

These observations suggest that the synergistic antitumoral effects of the combination might result from upregulation of the well-established HDAC inhibitor target p21. To verify the functional significance of p21 induction for enhanced apoptotic response, we prevented p21 accumulation using RNAi and compared the level of apoptosis upon VPA/PKC412 exposure to control siRNA treated cells. As shown in Figure 2d the extent of PARP cleavage upon combination treatment increased to a ratio of 0.4 compared to 0.3 observed for PKC412 only treatment . In p21-depleted cells this ratio remained unchanged at 0.3 indicating that p21 depletion prevents VPA from enhancing PKC412-induced apoptosis ($p=0.0133$). Collectively, these data suggest that induction of p21 by VPA is an important component contributing to enhanced apoptosis upon cotreatment with PKC412.

PAX3/FKHR mediates repression of p21.

Because a number of oncogenes repress p21 to promote tumorigenesis (as reviewed in (Gartel and Radhakrishnan, 2005)), we sought to determine whether also the PAX3/FKHR oncogene exerts a suppressive effect on p21 expression. Hence, we silenced endogenous PAX3/FKHR in aRMS cells

and measured p21 protein levels. As shown in Figure 3a and Supplementary Figure S2 reduced PAX3/FKHR levels led to dramatic increase in p21 protein expression in a panel of aRMS cell lines.

To further validate PAX3/FKHR as a negative regulator of p21 expression, we examined its effect directly on the p21 promoter by luciferase reporter assays. Transfection of 293T cells with a PAX3/FKHR vector decreased p21 promoter driven luciferase expression to 26% (Figure 3b).

As PAX3/FKHR interferes with expression of p21 and aRMS cells undergo apoptosis on silencing of PAX3/FKHR by oligonucleotides (Bernasconi *et al.*, 1996) or siRNA (Ebauer *et al.*, 2007), we assessed the relevance of p21 induction for this apoptotic response by cotransfecting RH4 cells with siRNAs against p21 and PAX3/FKHR. Compared to control or p21 siRNA transfected cells, which only show ratios of cleaved to uncleaved PARP of 0.1 and 0.07 respectively, PAX3/FKHR siRNA transfected cells demonstrate strongly enhanced PARP cleavage (0.43). Importantly, this apoptotic response to PAX3/FKHR silencing was rescued upon codepletion of p21 as indicated by a reduction of PARP cleavage ratio to 0.18 (Figure 3c). These results demonstrate that PAX3/FKHR represses p21 levels and suggest that upregulation of p21 in response to PAX3/FKHR downregulation is necessary for efficient induction of apoptosis.

PAX3/FKHR controls expression of p21 via EGR1

Because inhibition of DNA-binding of PAX3/FKHR by PKC412 (Amstutz *et al.*, 2008) was not able to induce p21 expression (Figure 2d) we reasoned that PAX3/FKHR might regulate p21 gene expression at levels other than transcription. Recently, it has been demonstrated that PAX3/FKHR can interact with and mediate destabilization of the transcription factor EGR1 ((Roeb *et al.*, 2007) and Supplementary Figures S3a and b) which itself can directly modulate gene expression of p21 ((Choi *et al.*, 2008; Ragione *et al.*, 2003) and Supplementary Figure S3c)). These findings suggest that repression of p21 by PAX3/FKHR might be mediated by degradation of the transcription factor EGR1.

To address this hypothesis, we first examined the expression levels of p21 and EGR1 in control human myoblasts and a series of aRMS tumor cell lines by immunoblot analysis. These experiments revealed a significant decrease in both p21 and EGR1 protein expression levels in aRMS cell lines in comparison to control myoblasts (Figure 4a).

Proteasome inhibition by MG132 prevents EGR1 destabilization by exogenous PAX3/FKHR in 293T cells ((Roeb *et al.*, 2007) and Supplementary Figure S3b.) Therefore, we treated aRMS cells with MG132. This caused a dose-dependent increase both of EGR1 and p21 protein levels (Figure. 4b). As

p21 itself is subject to ubiquitination, this increase most likely results from increased p21 protein stability rather than elevated transcription levels induced by EGR1. In order to investigate the relevance of EGR1-destabilization by PAX3/FKHR on p21 transcription, we performed luciferase reporter assays using a p21-promoter deletion construct lacking the distal p53 consensus binding site. As shown in Figure 4c in 293T cells, p21 promoter activity increased with the amount of transfected EGR1, suggesting that EGR1 can induce p21 transcription independent of p53. Moreover, coexpression of PAX3/FKHR inhibits EGR1 activation of the p21 promoter in a dose-dependent fashion. Interestingly, this inhibition could be partially rescued by treatment with increasing amounts of MG132 (Figure 4d and Supplementary Figure S3b). This suggests that p21 protein levels are controlled in aRMS cells via transcriptional activation by EGR1 which itself is destabilized by PAX3/FKHR.

To further validate this hypothesis, we assessed whether silencing of EGR1 influences p21 expression levels. As shown in Figure 4a, untreated RH4 cells express only low levels of endogenous EGR1 protein. Moreover, further depletion by RNAi mediated yet a reduction of p21 expression which was proportional to EGR1 knockdown efficiency (Figure 4e and Supplementary Figure S3d). In addition, silencing of PAX3/FKHR mediated an increase in EGR1 as well as p21 protein levels. These data are consistent with the notion that EGR1 regulates p21 transcription and that upon knockdown of PAX3/FKHR, EGR1 is no longer subject to proteasomal degradation and hence able to transcriptionally activate p21.

PKC412/VPA combination treatment results in reactivation of p21 expression levels and enhanced antitumoral action *in vivo*.

To investigate the value of combination therapy *in vivo*, we used an aRMS xenograft mouse model generated by subcutaneous injection of RH4 cells into immunocompromised (nu/nu) mice. As shown in Figure 5a, daily administration of VPA (400 mg/kg) or PKC412 (100 mg/kg) alone for a 7-day time period was able to reduce tumor growth by about 50%. Interestingly, combination treatment reduced tumor growth by a further 3-4 fold compared to either single treatment alone.

In line with our *in vitro* results, immunohistochemical analysis of tumor sections revealed that VPA treatment alone or in combination with PKC412 led to elevated levels of p21 protein *in vivo* (Figure 5b). In addition, analysis of tumors subjected to each single treatment showed that VPA had only a minimal effect on proliferation whereas PKC412 treatment caused a 25% reduction in the number of

proliferative cells (Figure 5c). Both single treatments also led to a 2-fold increase in the number of apoptotic cells compared to placebo treated tumors (Figure 5d). Importantly however, combination therapy resulted in both strongest decrease in proliferation (by 40%) and highest number of apoptotic cells (72 cells/visual field) compared to placebo treatment (11 cells/visual field) (Figures 5C and D). In summary, these results suggest that also *in vivo* reactivation of p21 contributes to augment PKC412 mediated antitumorigenic activity and therefore highlight a PKC412/VPA combination treatment as a evidence-based novel treatment strategy for aRMS.

Discussion

aRMS represents a therapeutic challenge because of its frequent resistance to conventional chemotherapy. Especially relapsed aRMS patients have a very poor prognosis (Pappo *et al.*, 1999; Raney *et al.*, 2001). Therefore, the development of novel treatment modalities in necessary to improve the clinical outcome for aRMS patients.

Recently, we identified the kinase inhibitor PKC412 to exert a potent antitumor effect in aRMS *in vitro* and *in vivo* by reducing the transcriptional activity of the PAX3/FKHR oncogene (Amstutz *et al.*, 2008). However, to minimize the potential development of resistance and further improve efficacy the use of drug combinations is a well-established pharmaceutical principle. Since numerous novel agents are now being developed for clinical testing this creates almost limitless possibilities of combination regimens. Therefore, development of strategies to identify the most promising combinations will become very important.

Here, we demonstrate that the HDAC inhibitor VPA, a well-established drug used in therapy for seizures and bipolar disorders, acts as a potent combination partner for PKC412 to mediate increased induction of apoptosis in aRMS cells, both *in vitro* and *in vivo*. Interestingly, combinations with standard cytotoxic drugs used in RMS treatment showed only minimal synergistic effects. This is in contrast to acute myeloid leukaemia (AML) for which PKC412 is currently evaluated in phase II clinical trials, as combinations with conventional antileukemic agents demonstrate superior anti-cancer activity for FLT3 mutation-positive AML compared to single treatment alone (Furukawa *et al.*, 2007). Only one study in AML suggested that HDAC inhibitors could be used effectively in combination with PKC412 (Bali *et al.*, 2004).

In vivo, further reduction in tumor growth by the combination was observed after a short treatment period of only seven days. It will be interesting to evaluate this combination in respect to other targeted drugs that have been suggested as novel drugs for therapy of rhabdomyosarcoma, such as for example agents inhibiting the IGF-1R pathway (Cao *et al.*, 2008; Kolb *et al.*, 2008).

We provide evidence that VPA exerts its synergistic anti-cancerous activity on aRMS cells by mediating reactivation of p21 expression levels, again both *in vitro* and *in vivo*. Interestingly, this effect could also be observed with other HDAC inhibitors and was not restricted to VPA. Epigenetic repression of p21 has recently been shown to occur via HDAC4-mediated reduced acetylation of

Sp1/Sp3-binding sites at the proximal promoter of p21 in a human glioblastoma model (Mottet *et al.*, 2009). This effect was shown to be p53-independent which is similar to the results obtained here since aRMS cell lines used in this study are either depleted of mutated in p53 (Barlow *et al.*, 2006) and the p21 reporter construct did not include p53 binding sites. Hence, transcriptional repression of p21 might occur through HDAC4 also in the rhabdomyosarcoma model and the use of more specific HDAC4 inhibitors might further enhance the specificity of our treatment strategy.

Since p21 levels in aRMS are usually low (Figures 3 and 4), an important goal was to identify the relevant mechanisms of repression. Interestingly, we found that p21 expression is strongly upregulated upon silencing of PAX3/FKHR. In addition, efficient induction of apoptotic aRMS cell death upon PAX3/FKHR depletion occurs, at least in part, through p21 since its depletion can rescue from apoptosis. Given that PAX3/FKHR can destabilize the transcription factor EGR1 (Roeb *et al.*, 2007; Roeb *et al.*, 2008) and that EGR1 itself was shown to modulate p21 transcription (Ragione *et al.*, 2003), we hypothesized that EGR1 is critically involved in p21 activation upon PAX3/FKHR depletion. This conclusion is supported by several lines of evidence: First, EGR1 and p21 protein expression levels are reduced in a series of translocation positive aRMS tumor cell lines as compared to human myoblasts. Second, enhanced induction of p21 reporter activity upon EGR1 overexpression was strongly inhibited by cotransfection with PAX3/FKHR. Third, this inhibition could be prevented by treatment with the proteasome inhibitor MG132. Finally, silencing of endogenous PAX3/FKHR induced protein expression of both EGR1 as well as its transcriptional target p21. Hence, we identified with p21, apart from p57 (Roeb *et al.*, 2007), a second important target gene which is transcriptionally modulated by destabilization of EGR1 through PAX3/FKHR thereby also validating this newly described role of PAX3/FKHR in aRMS tumor cells (Roeb *et al.*, 2007). These data indicate that aRMS tumor cells exert both epigenetic regulatory strategies and destabilization of the transcription factor EGR1 as complementing mechanisms to ensure downregulation of p21, indicating a potential tumor suppressing function for p21 also in aRMS pathology.

These data also suggest novel treatment possibilities for aRMS tumors: One rationale might be to explore the proteasome as a target of potential therapeutic value. However, as it could be shown that PAX3/FKHR rather than EGR1 is ubiquitinated (Roeb *et al.*, 2008), strategies that exploit proteasome inhibition might also lead to increased protein levels of transcriptional active PAX3/FKHR in aRMS tumor cells. Therefore, we propose combination strategies of PKC412 with HDAC inhibitors such as VPA, as this cotreatment results in reactivation of the EGR1 target p21 and in reduction of the

transcriptional activity of PAX3/FKHR. Thus, the molecular mechanism of this synergistic combination is most likely based on targeting both the transcriptional and protein-degradation activity of the PAX3/FKHR oncogene (Figure 6). As both therapeutic agents used for the combination treatment are broad spectrum drugs, it is likely that other so far not identified mechanisms might contribute to their activity. Nevertheless, the use of HDAC isoform specific inhibitors combined with more specific kinase inhibitors (after identification of the signalling pathway responsible for PAX3/FKHR phosphorylation) might provide additional specificity to this treatment strategy. Whether this would also translate to enhanced clinical benefits, remains to be investigated.

Altogether, our study provides novel insights into the oncogenic mechanisms of PAX3/FKHR and marks the combination of VPA and PKC412 as an evidence-based alternative to standard chemotherapy protocols for poorly prognosed aRMS patients.

Materials and Methods

Cell lines and pharmacologic inhibitors. Alveolar rhabdomyosarcoma cell lines RH4 and RH28 were kindly provided by Peter Houghton (St. Jude Children's Hospital, Memphis, TN, USA) and RMS13 were obtained from the Ludwig-Maximillans-University (Munich, Germany). RH30 as well as 293T cells were purchased from the American Type Culture collection (ATCC, LGC Promochem, Molsheim Cedex, France). A33 and B6M myoblasts were established in our laboratories (Genini *et al*., 1996). SkM1 and SkM2 myoblasts were purchased from Promocell (Allschwil, Switzerland). Etoposide, Vincristine, Carboplatin, Natrium Butyrate and VPA were purchased from Sigma (Buchs, Switzerland). Daunorubicine (Cerubidine®) was obtained from Sanofi-Aventis (Geneva, Switzerland), Topotecan from Glaxo Smith Kline (Münchenbuchsee, Switzerland) and SAHA from Alexis Biosciences (Lausen, Switzerland). PKC412 was kindly provided by Novartis (Basel, Switzerland).

***In vitro* combination studies.** IC_{50} values of drugs alone or in combination with 50nM PKC412 were determined by MTT assays (Roche, Basel, Switzerland) according to the manufacturer's protocol. 10 000 cells per well of a 96-well plate were treated with increasing concentrations of Daunorubicine (0 - 3 µM), Etoposide (0 - 30 µM), Topotecan (0 - 10 µM), Vincristine (0 - 5 nM), Carboplatin (0 - 1 mM), VPA (0 - 30 mM) or SAHA (0 - 6 µM) in a final volume of 100 µl for 96 hours. For each concentration, the percent viable cells compared to control was plotted against the logarithm of drug concentrations. IC_{50} values were then calculated by nonlinear regression curve fitting using GraphPad Prism software (GraphPad Software Inc., San Diego, CA, USA).

Trypan Blue Exclusion. The dye (Sigma, Buchs, Switzerland) exclusion test was used to determine the number of viable and dead cells present in trypsinized cell suspensions upon inhibitor treatment.

Caspase-3 assay. Activated caspase-3 levels were detected by CaspGLOW Red Active Caspase-3 staining kit (BioVision, Amsbio, Lugano, Switzerland) according to the manufacturer's instruction. Cells were treated with inhibitors for 48h. Active caspase-3 positive cells were determined by fluorescence microscopy. For each treatment, a minimum of 500 cells were counted.

Immunoblotting. Proteins were separated using a NuPAGE electrophoresis system (Invitrogen, Basel Switzerland). Western blots were probed using primary antibodies against poly(ADP-ribose) polymerase (PARP, 1:1000), p53 (1:1000), $p21^{Waf1/Cip1}$ (12D1, 1:1000, all from Cell Signaling Technology, Allschwil, Switzerland), EGR1 (588, sc-110, 1:500,Santa Cruz Biotechnology, Heidelberg, Germany), FKHR (C20; 1:500; Santa Cruz Biotechnology, Heidelberg, Germany) and β-actin (A2103; 1:1000; Sigma, Buchs, Switzerland).

siRNA-mediated silencing. Cells were transfected with either PAX3/FKHR break-point specific siRNA (Kikuchi *et al.*, 2008), p21 siRNA, EGR1#1 siRNA or scrambled negative control (AllStars) siRNA (all obtained from Qiagen except for EGR1#2 from Ambion) for 48h using N-ter nanoparticle transfection reagent (Sigma-Aldrich, Buchs, Switzerland) according to the manufacturer's instructions. For knockdown experiments in combination with PKC412/VPA treatment, cells were incubated with siRNA for 40h and subsequently exposed to treatment for additional 8h.

Proteasome inhibition assays. RH4 cells were treated with MG132 (VWR international AG, Dietikion, Switzerland) dissolved in DMSO or DMSO alone for 3h. For proteasome inhibition during luciferase assay experiments 293T cells were treated with indicated concentrations of MG132 sixteen hours before harvesting.

Transactivation assays and plasmids. The PAX3/FKHR construct together with a reporter plasmid containing the luciferase gene downstream of a p21 promoter fragment that spans nt -150 to +39 and lacks the p53 binding site (p21-Luc (-150/+38), (Kim and Rossi, 2007)) and a plasmid containing the lacZ gene were transfected into 293T cells. For EGR1 destabilization assays 293T cells were in addition to these plasmids cotransfected with increasing quantities of EGR1 plasmid. Total DNA mass was kept constant by the addition of pcDNA3.1. Where indicated, cells were treated with MG132, followed by lysis in reporter lysis buffer (Promega, Wallisellen, Switzerland). β-Galactosidase and luciferase activities were determined with the corresponding assay systems (Promega, Wallisellen, Switzerland) and luciferase activity values were normalized with the β-galactosidase activity values.

Treatment of aRMS xenograft mice. 10^7 RH4 cells resuspended in 100 µl of PBS, were subcutaneously injected into the right flank of female CD-1 athymic nude mice (nu/nu) (Charles River,

Germany). When tumors reached a volume of approximately 125 mm^3, mice were treated with 100 mg/kg/day PKC412, 100 mg/kg/day PKC412 and 400 mg/kg/day VPA, 400 mg/kg/day VPA or placebo. Treatment was performed for 7 consecutive days. Tumor size was determined every 3 days by measuring two diameters (d_1, d_2) in right angles using a calliper. Tumor volumes were calculated using the formula $V = (4/3)\ \pi\ r^3$ ($r = (d_1 + d_2)/4$). PKC412, formulated in a microemulsion (Novartis, Basel, Switzerland), was applied orally according to the guidelines of Novartis (Basel, Switzerland). Valproic acid, dissolved in PBS, was administered intraperitoneally. Every treatment group consisted of 5 animals.

Immunohistochemistry. For histologic analysis, 3 mice per treatment group were sacrificed at the end of the *in vivo* experiment treatment period (day 25). Tumors were isolated, fixed in 4 % paraformaldehyde in PBS and paraffin embedded. Tumor sections were subjected to stainings with rabbit-polyclonal p21 antibody using standard histological techniques. TUNEL analysis was performed according to the manufacturer's instructions (Roche, Basel, Switzerland). Furthermore, tumor sections were stained for the proliferation marker Ki-67 by using a monoclonal rabbit Ki-67 antibody (NeoMarkers, Fremont, CA, USA) and the Ventana iView DAB Detection Kit. TUNEL- or Ki-67-positive cells were counted in 12 randomly selected visual fields at x100 magnification (634.2 µm x 476.5 µm).

Conflict of interest

The authors declare no conflict of interest.

Acknowledgments.

We thank professor Soon Young Shin for providing constructs encoding EGR1 and p21 luciferase reporter plasmid, Silvia Behnke for her help with the stainings of tumor sections and Sarah Steinbacher for her graphical support in designing Figure. 6. This work was supported by grants (3100-109837 and 3100-122562) from the Swiss National Science Foundation (SNF).

Supplementary information is available at the Oncogene website (http://www.nature.com/onc)

References

Amstutz R, Wachtel M, Troxler H, Kleinert P, Ebauer M, Haneke T *et al.* (2008). Phosphorylation regulates transcriptional activity of PAX3/FKHR and reveals novel therapeutic possibilities. *Cancer Res* **68**: 3767-76.

Archer SY, Meng S, Shei A and Hodin RA. (1998). p21(WAF1) is required for butyrate-mediated growth inhibition of human colon cancer cells. *Proc Natl Acad Sci U S A* **95**: 6791-6.

Bali P, George P, Cohen P, Tao J, Guo F, Sigua C *et al.* (2004). Superior activity of the combination of histone deacetylase inhibitor LAQ824 and the FLT-3 kinase inhibitor PKC412 against human acute myelogenous leukemia cells with mutant FLT-3. *Clin Cancer Res* **10**: 4991-7.

Barlow JW, Wiley JC, Mous M, Narendran A, Gee MF, Goldberg M *et al.* (2006). Differentiation of rhabdomyosarcoma cell lines using retinoic acid. *Pediatr Blood Cancer* **47**: 773-84.

Bernasconi M, Remppis A, Fredericks WJ, Rauscher FJ, 3rd and Schafer BW. (1996). Induction of apoptosis in rhabdomyosarcoma cells through down-regulation of PAX proteins. *Proc Natl Acad Sci U S A* **93**: 13164-9.

Breneman JC, Lyden E, Pappo AS, Link MP, Anderson JR, Parham DM *et al.* (2003). Prognostic factors and clinical outcomes in children and adolescents with metastatic rhabdomyosarcoma--a report from the Intergroup Rhabdomyosarcoma Study IV. *J Clin Oncol* **21**: 78-84.

Cao L, Yu Y, Darko I, Currier D, Mayeenuddin LH, Wan X *et al.* (2008). Addiction to elevated insulin-like growth factor I receptor and initial modulation of the AKT pathway define the responsiveness of rhabdomyosarcoma to the targeting antibody. *Cancer Res* **68**: 8039-48.

Choi BH, Kim CG, Bae YS, Lim Y, Lee YH and Shin SY. (2008). p21 Waf1/Cip1 expression by curcumin in U-87MG human glioma cells: role of early growth response-1 expression. *Cancer Res* **68**: 1369-77.

Ebauer M, Wachtel M, Niggli FK and Schafer BW. (2007). Comparative expression profiling identifies an in vivo target gene signature with TFAP2B as a mediator of the survival function of PAX3/FKHR. *Oncogene* **26**: 7267-81.

Furukawa Y, Vu HA, Akutsu M, Odgerel T, Izumi T, Tsunoda S *et al.* (2007). Divergent cytotoxic effects of PKC412 in combination with conventional antileukemic agents in FLT3 mutation-positive versus -negative leukemia cell lines. *Leukemia* **21**: 1005-14.

Gartel AL and Radhakrishnan SK. (2005). Lost in transcription: p21 repression, mechanisms, and consequences. *Cancer Res* **65**: 3980-5.

Genini M, Schwalbe P, Scholl FA and Schafer BW. (1996). Isolation of genes differentially expressed in human primary myoblasts and embryonal rhabdomyosarcoma. *Int J Cancer* **66**: 571-7.

Kikuchi K, Tsuchiya K, Otabe O, Gotoh T, Tamura S, Katsumi Y *et al.* (2008). Effects of PAX3-FKHR on malignant phenotypes in alveolar rhabdomyosarcoma. *Biochem Biophys Res Commun* **365**: 568-74.

Kim DH and Rossi JJ. (2007). Strategies for silencing human disease using RNA interference. *Nat Rev Genet* **8**: 173-84.

Kim JS, Lee S, Lee T, Lee YW and Trepel JB. (2001). Transcriptional activation of p21(WAF1/CIP1) by apicidin, a novel histone deacetylase inhibitor. *Biochem Biophys Res Commun* **281**: 866-71.

Kolb EA, Gorlick R, Houghton PJ, Morton CL, Lock R, Carol H *et al.* (2008). Initial testing (stage 1) of a monoclonal antibody (SCH 717454) against the IGF-1 receptor by the pediatric preclinical testing program. *Pediatr Blood Cancer* **50**: 1190-7.

Liu C, Adamson E and Mercola D. (1996). Transcription factor EGR-1 suppresses the growth and transformation of human HT-1080 fibrosarcoma cells by induction of transforming growth factor beta 1. *Proc Natl Acad Sci U S A* **93**: 11831-6.

Merlino G and Helman LJ. (1999). Rhabdomyosarcoma--working out the pathways. *Oncogene* **18**: 5340-8.

Meyer WH and Spunt SL. (2004). Soft tissue sarcomas of childhood. *Cancer Treat Rev* **30**: 269-80.

Mottet D, Pirotte S, Lamour V, Hagedorn M, Javerzat S, Bikfalvi A *et al.* (2009). HDAC4 represses p21(WAF1/Cip1) expression in human cancer cells through a Sp1-dependent, p53-independent mechanism. *Oncogene* **28**: 243-56.

Pappo AS, Anderson JR, Crist WM, Wharam MD, Breitfeld PP, Hawkins D *et al.* (1999). Survival after relapse in children and adolescents with rhabdomyosarcoma: A report from the Intergroup Rhabdomyosarcoma Study Group. *J Clin Oncol* **17**: 3487-93.

Ragione FD, Cucciolla V, Criniti V, Indaco S, Borriello A and Zappia V. (2003). p21Cip1 gene expression is modulated by Egr1: a novel regulatory mechanism involved in the resveratrol antiproliferative effect. *J Biol Chem* **278**: 23360-8.

Raney RB, Anderson JR, Barr FG, Donaldson SS, Pappo AS, Qualman SJ *et al.* (2001). Rhabdomyosarcoma and undifferentiated sarcoma in the first two decades of life: a selective review of intergroup rhabdomyosarcoma study group experience and rationale for Intergroup Rhabdomyosarcoma Study V. *J Pediatr Hematol Oncol* **23**: 215-20.

Roeb W, Boyer A, Cavenee WK and Arden KC. (2007). PAX3-FOXO1 controls expression of the p57Kip2 cell-cycle regulator through degradation of EGR1. *Proc Natl Acad Sci U S A* **104**: 18085-90.

Roeb W, Boyer A, Cavenee WK and Arden KC. (2008). Guilt by association: PAX3-FOXO1 regulates gene expression through selective destabilization of the EGR1 transcription factor. *Cell Cycle* **7**: 837-41.

Smith LM, Anderson JR, Qualman SJ, Crist WM, Paidas CN, Teot LA *et al.* (2001). Which patients with microscopic disease and rhabdomyosarcoma experience relapse after therapy? A report from the soft tissue sarcoma committee of the children's oncology group. *J Clin Oncol* **19**: 4058-64.

Sowa Y, Orita T, Minamikawa S, Nakano K, Mizuno T, Nomura H *et al.* (1997). Histone deacetylase inhibitor activates the WAF1/Cip1 gene promoter through the Sp1 sites. *Biochem Biophys Res Commun* **241**: 142-50.

Wilson AJ, Byun DS, Popova N, Murray LB, L'Italien K, Sowa Y *et al.* (2006). Histone deacetylase 3 (HDAC3) and other class I HDACs regulate colon cell maturation and p21 expression and are deregulated in human colon cancer. *J Biol Chem* **281**: 13548-58.

Figure legends

Figure 1 Screening for combination partners identifies VPA to mediate increased PKC412 drug efficacy. (**a**) aRMS cell lines were treated with increasing concentrations of chemotherapeutic drugs and HDAC inhibitors for 96h either alone or in combination with 50nM PKC412. Cytotoxicity was determined by using MTT assays and IC_{50} values were calculated by nonlinear regression curve fitting. Ratios of combined versus non-combined treatments <1.0 correspond to synergistic interactions. Columns, mean of three independent experiments performed in triplicate; bars, SD. (**b**) aRMS cell lines were exposed to the indicated concentrations of PKC412 and/or VPA for 24 - 72h and cell viability (%) was assessed using trypan blue exclusion. Points, mean of three independent experiments; bars, SD.

Figure 2 Cotreatment with VPA enhances apoptotic response to PKC412 in aRMS cells. Apoptotic RH4 (**a**) and RH30 (**b**) cells were detected as caspase-3-positive cells under fluorescence microscopy and indicated as % stained cells (right). Columns, mean of three independent experiments; bars, SD. (**c**) Western blot analysis of PARP cleavage after indicated hours of treatment with 0.5µM PKC412 (P), 1 mM VPA (V) alone or in combination (P+V) compared to DMSO–treated (D) controls. (**d**) After 40h of silencing with p21-targeting or scrambled siRNA, RH4 cells were treated with 0.5µM PKC412 (P), 1mM VPA (V) alone or in combination (P+V) or DMSO (D) for 8h. Quantification of PARP cleavage detected by Western blotting was performed using densitometry and ratios of cleaved to uncleaved PARP are indicated (results are representative of three independent experiments). p21 depletion was verified by Western blotting.

Figure 3 p21 expression is upregulated upon silencing of PAX3/FKHR and contributes to efficient induction of apoptosis. (**a**) RH4 cells were transiently transfected with scrambled (sc) or PAX3/FKHR (P3F) specific siRNA and expression of p21 and PAX3/FKHR was determined by Western blot analysis. (**b**) Luciferase reporter assay of 293T cells cotransfected with p21 promoter-reporter plasmid and PAX3/FKHR (P3F) expression plasmid or empty vector control. Columns, mean of three independent experiments; bars, SD. (**c**) RH4 cells were transfected with a combination of siRNAs targeting PAX3/FKHR and p21 and compared to single or scrambled siRNA treated cells.

Concentrations of siRNA applied for each target were 25 nM and total siRNA concentrations were kept constant (50 nM) by addition of sc siRNA. PARP cleavage was analysed by Western blotting. Bands representing cleaved and uncleaved PARP were quantified by densitometry. Knockdown efficiency and effects of silencing were assessed by Western blot analysis of p21 and PAX3/FKHR.

Figure 4 PAX3/FKHR regulates p21 expression via EGR1. (**a**) Expression levels of p21 and EGR1 were examined by Western blotting of myoblasts and a series of aRMS cell lines. For statistical analysis bands were quantified by densitometry and the resulting expression values for EGR1 and p21 were compared between myoblasts and aRMS cells, *P< 0.05. (**b**) Western blot analysis of EGR1 and p21 expression in RH4 cells treated with increasing concentrations of MG132. (**c**) Luciferase reporter assay of the p21 promoter-reporter plasmid with increasing quantities of EGR1 and PAX3/FKHR alone or (**d**) in the presence of increasing quantities of MG132. Columns, mean of three independent experiments; bars, SD. (**e**) RH4 cells were transfected with siRNAs targeting either EGR1(EGR1#1and#2), PAX3/FKHR or scrambled siRNA. Knockdown efficiencies and effects of silencing were assessed by Western blot analysis using antibodies against EGR1, PAX3/FKHR and p21.

Figure 5 Combination with VPA augments the antitumoral action of PKC412 and induces p21 *in vivo*. (**a**) Growth curves of aRMS xenografts in nude mice treated either with the combination of 100 mg/kg/day PKC412 and 400 mg/kg/day VPA or with the single agents alone. Treatment was performed from daily during the first 7 days; n = 5. Bar graph shows the tumor growth of treated tumors at day 25. Points, means; bars, SD. (**b**) Representative immunohistochemical analysis of p21, (**c**) Ki-67 and (**d**) TUNEL stainings of tumors isolated at the end of the *in vivo* experiment (day 25) from each experimental group. Ki-67- and TUNEL-positive cells were scored under light microscopy at x100 fold magnification as shown in this figure ; n = 3. Columns, means; bars, SD. *P < 0.05, **P < 0.01 and ***P < 0.001 compared with placebo-treated mice; §P < 0.05 and §§P < 0.01 compared with VPA-treated mice; ††P < 0.01 compared with PKC412-treated mice.

Figure 6 Schematic representation of the molecular interactions described in this study. Briefly, phosphorylation regulates the transcriptional activity of PAX3/FKHR (Amstutz *et al.*, 2008) whereas

ubiquitination of PAX3/FKHR mediates codegradation of the transcription factor EGR1 (Roeb *et al.*, 2007) thereby reducing p21 expression levels. Therefore, the combination of VPA and PK412 may provide a therapeutic benefit in the treatment of aRMS through the abrogation of different levels of PAX3/FKHR oncogenic activity.

Hecker, Figure 1

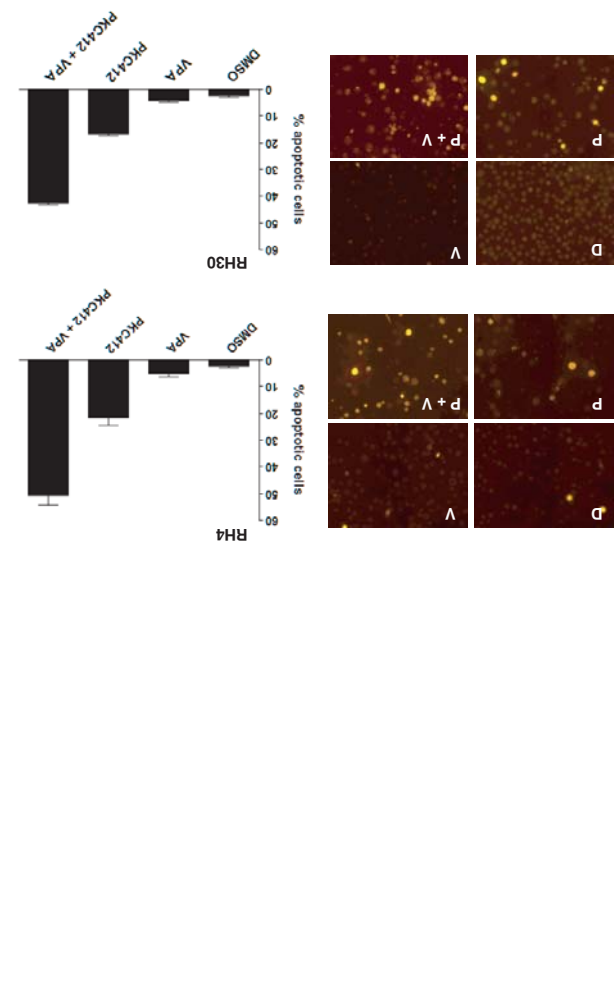

Hecker, Figure 2

Hecker, Figure 3

Hecker, Figure 4

Hecker, Figure 5

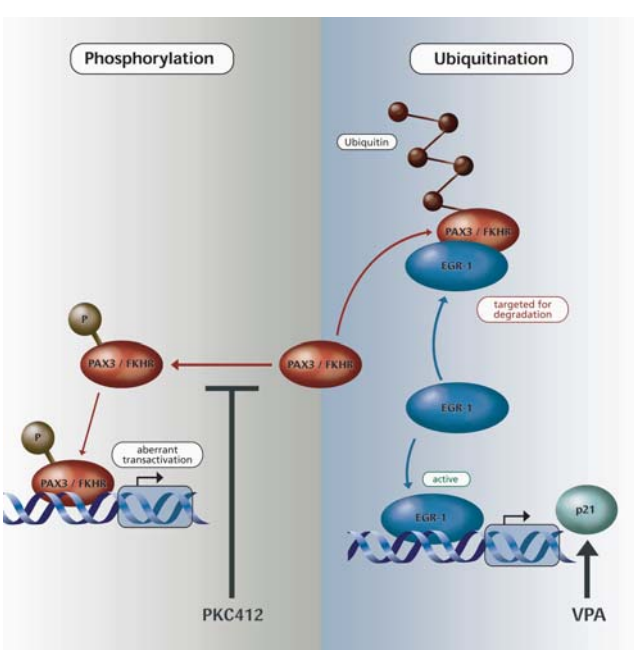

Hecker, Figure 6

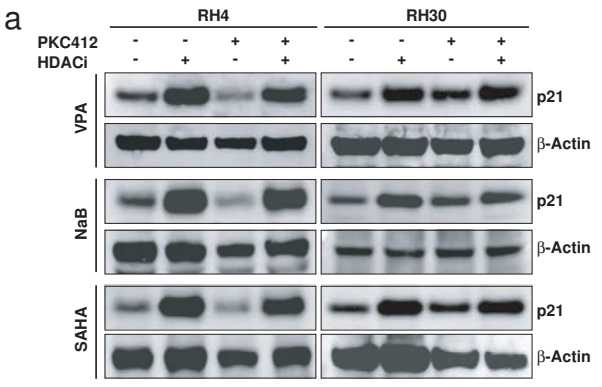

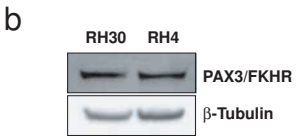

Hecker, Supplementary Figure S1

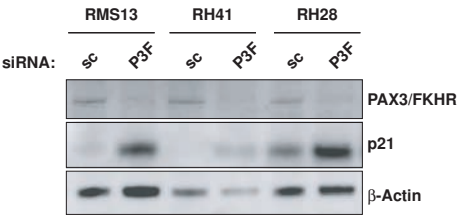

Hecker, Supplementary Figure S2

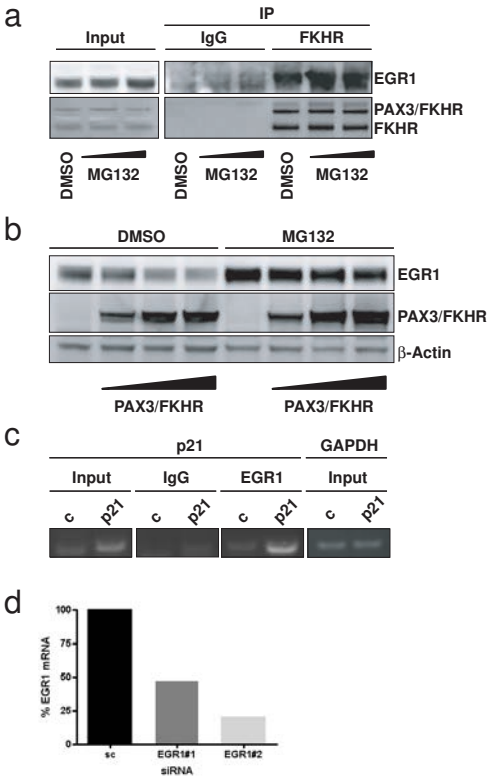

Hecker, Supplementary Figure S3

Supplementary Figure S1 (**a**) HDAC inhibitors upregulate p21 expression levels in aRMS tumor cells irrespective of additional PKC412 treatment. Western blot analysis of p21 expression levels in RH4 and RH30 tumor cells treated with three different HDAC inhibitors either in the presence or absence of PKC412 as indicated. β-Actin was used as a loading control. (**b**) Western blot analysis of PAX3/FKHR expression in both aRMS cell lines, RH30 and RH4.

Supplementary Figure S2 p21 protein levels are upregulated upon silencing of PAX3/FKHR in a panel of additional aRMS cell lines. aRMS cell lines RH13, RH41 and RH28 were transiently transfected with scrambled (sc) or PAX3/FKHR (P3F) breakpoint-specific siRNA for 48 h. PAX3/FKHR fusion status of all cell lines and successful knockdown were demonstrated by Western blot analysis of PAX3/FKHR. Upregulation of p21 protein levels upon PAX3/FKHR knock-down in all aRMS cell lines tested supports the importance of p21 downregulation for PAX3/FKHR oncogenicity.

Supplementary Figure S3 PAX3/FKHR not only interacts with EGR1 but also mediates its degradation thereby controlling p21 expression levels. (**a**) Co-immunoprecipitation analysis of endogenous EGR1 and PAX3/FKHR from RH4 cells in the presence or absence of increasing amounts of MG132. (**b**) Western blot analysis of EGR1 upon co-transfection of same amounts of EGR1 and increasing amounts of PAX3/FKHR expression plasmids. In the absence of MG132 co-transfection of increasing amounts of PAX3/FKHR reduce EGR1 protein levels in a dose-dependent manner which can be partially rescued by the proteasome inhibitor MG132; these data complement the results shown in Figure 4c and d, respectively. (**c**) Binding of EGR1 to the either the endogenous p21 promoter (control sample, c) as well as to p21 promoter region of the p21 (-150/+39) construct as detected by chromatin immunoprecipitation (ChIP). Protein/DNA complexes were immunoprecipitated with EGR1 antibody or unspecific mouse IgG. The figure shows PCR amplicons of a p21 promoter fragment of unprecipitated (input) or precipitated DNA. GAPDH amplification of unprecipitated material was used to control the amount of input material. (d) Quantification of the knockdown efficiency of two different siRNAs targeting EGR1 by qRT–PCR analysis. Relative percentage of EGR1 mRNA compared to scRNA-treated cells (100%) are shown. As seen in Figure 4e the increasing EGR1 knockdown efficiency also persists on protein levels and likewise results in a graded reduction of p21 protein levels.

Supplementary Materials and Methods

Real-time PCR. Quantitative reverse transcription-PCR (qRT-PCR) was performed under universal cycling variables on an ABI 7900HT instrument using commercially available target probes and Mastermix (all from Applied Biosystems, Rotkreuz, Switzerland). Detection of EGR1 was achieved using a specific Taqman Gene Expression Assay (Hs00152928_m1). Cycle threshold (C_T) values were normalized to glyceraldehyde-3-phosphate dehydrogenase (GAPDH). Relative expression levels of the target gene upon siRNA mediated knockdown were calculated using the C_T method.

Chromatin immunoprecipitation (ChIP) assay. ChIP was performed using a commercially available ChIP-IT enzymatic kit (Active Motif, Rixensart, Belgium) according to manufacturer's instructions. 293T cells were co-transfected with either empty vector (pGl4.17, Promega, Wallisellen, Switzerland) or pGl4.17 vector containing the p21 promoter fragment that spans nt -150 to +39 (29). DNA-bound protein was immunoprecipitated using an anti-EGR1 (Santa-Cruz Biotechnology, Heidelberg, Germany) antibody or mouse IgG (Active Motif, Rixensart, Belgium) as negative control. For quantification of co-precipitated DNA, samples were than subjected to amplification by employing primers (For: 5'-AGCTGGCTCGGCGCTGGGCA-3'; and Rev: 5'- GCGGCCCTGATATACAACC-3') which amplified the promoter region (130 bp) of p21. Amplification of glyceraldehyde-3-phosphate dehydrogenase (GAPDH) form the unprecipitated chromatin was used to control the amount of input material.

Co-immunoprecipitation (Co-IP). Co-immunoprecipitation of endogenously expressed proteins was performed using RH4 cells either incubated with DMSO or incubated with the indicated amount of MG132 for 2 hours. Cells were harvested in 1%NP40 lysis buffer. Extracts were incubated overnight with 2.5 µg of anti-FKHR (Santa Cruz Biotechnology, Heidelberg, Germany) antibody in the presence of Protein G beads using a Protein G Immunoprecipitation kit (Sigma-Aldrich, Buchs, Switzerland) and resulting complexes were washed, denatured and eluted according to the manufacturer's instruction.

EGR1-PAX3/FKHR- Co-Transfection Assay. 293T cells were co-transfected with a constant amount of EGR1 plasmid together with increasing amounts of PAX3/FKHR plasmid. Total DNA mass was kept

constant by the addition of pcDNA3.1. Before harvesting, cells were either incubated with DMSO or 5μM MG132 dissolved in DMSO for 16 hours and the obtained extracts were subjected to western blot analysis.